

Analyst

Accepted Manuscript



This is an *Accepted Manuscript*, which has been through the Royal Society of Chemistry peer review process and has been accepted for publication.

Accepted Manuscripts are published online shortly after acceptance, before technical editing, formatting and proof reading. Using this free service, authors can make their results available to the community, in citable form, before we publish the edited article. We will replace this *Accepted Manuscript* with the edited and formatted *Advance Article* as soon as it is available.

You can find more information about *Accepted Manuscripts* in the [Information for Authors](#).

Please note that technical editing may introduce minor changes to the text and/or graphics, which may alter content. The journal's standard [Terms & Conditions](#) and the [Ethical guidelines](#) still apply. In no event shall the Royal Society of Chemistry be held responsible for any errors or omissions in this *Accepted Manuscript* or any consequences arising from the use of any information it contains.

1 **Preparation of core–shell magnetic ion-imprinted polymer by sol-gel process for**
2 **selective extraction of Cu(II) from herbal medicines**

3 Huan He^{1,5}, Deli Xiao^{2,5}, Jia He², Hui Li^{3,6*}, Hua He^{2,4,6*}, Hao Dai², Jun Peng²

4

5 1 State Key Laboratory of Pollution Control and Resource Reuse, School of the Environment,
6 Nanjing University, Nanjing, 210023, China

7 2 Department of Analytical Chemistry, China Pharmaceutical University, Nanjing 210009, China

8 3 Hepalink Pharmaceutical company, co., Ltd, Shenzhen 518000, China

9 4 State Key Laboratory of Natural Medicines, China Pharmaceutical University, Nanjing 210009,
10 China

11 5 These authors equally contributed to this work and should be considered co-first authors

12 6 These authors equally contributed to this work and should be considered co-corresponding
13 authors

14

15 * To whom correspondence should be addressed: China Pharmaceutical University, 24 Tongjia
16 Lane, Nanjing 210009, Jiangsu Province, China

17 Tel.: +86 025 83271505; fax: +86 025 83271505.

18 E-mail: dochehua@163.com, jcb315@163.com (Hua He), lihui870710@gmail.com (Hui Li)

19 **Abstract**

20 A novel magnetic surface ion-imprinted polymer (c-MMWCNTs-SiO₂-IIP) was firstly
21 synthesized by using c-MMWCNTs as the core, 3-ammonium propyltriethoxysilane (APTES) as
22 the functional monomer, tetraethylorthosilicate (TEOS) as the cross-linker and Cu(II) as the
23 template. c-MMWCNTs-SiO₂-IIP was evaluated for selective extraction of Cu(II) from herbal
24 medicines extraction by magnetic solid phase extraction (M-SPE) procedure. Factor affecting the
25 separation and preconcentration of the target heavy metal was pH. Under the optimized
26 experimental conditions, the adsorption kinetics and adsorption capacity of
27 c-MMWCNTs-SiO₂-IIP toward Cu(II) were estimated. The results indicated that the adsorption
28 mechanism was corresponding with the pseudo-second-order adsorption process with a
29 correlation coefficient ($R^2 = 0.985$), and the maximum adsorption capacity is 42.2 mg/g. The
30 relative selectivity factor (β) values of Cu(II)/Zn(II) and Cu(II)/Pb(II) were 38.5 and 34.5,
31 respectively. c-MMWCNTs-SiO₂-IIP was applied for extracting and detecting Cu(II) in herbal
32 medicine combined with flame atomic absorption spectrometer successfully with high recoveries
33 ranged from 95.6% to 108.4%.

34

35 **Keywords:** core-shell, c-MMWCNTs-SiO₂-IIP, sol-gel, Cu(II), magnetic solid phase extraction
36 (M-SPE)

37

38 1. Introduction

39 Herbal medicines have played an important role in a thousand years of Chinese history. Active
40 pharmaceutical ingredients (API) extracted from the herbal medicines and complementary
41 alternative medicines (CAM) have attracted extensive attention throughout the world.¹ However,
42 contaminants, such as herbicides, pesticides, microbes and heavy metals caused by the
43 surrounding environment have become a severe problem that makes it unsafe for disease curing
44 and ultimately prevents the exports of API and CAM. Clinical studies show that some heavy
45 metals are toxic, but the tolerable amount of heavy metals plays a role in assisting drug efficacy.
46 Therefore, accurate and efficient qualitative control of heavy metals in Chinese medicinal
47 materials is of great significance.

48 To screen for heavy metal contamination, several analytical methods, including AAS, ICP-MS,
49 HPLC and NAA, have been applied to determine the suspected heavy metal toxicity.²⁻⁴ Since
50 traditional adsorbents, such as Fe₃O₄ particle,⁵ carbon nanotubes⁶ and magnetic CNTs/Fe₃O₄
51 composites (c-MMWCNTs)^{7, 8} which bear no selectivity cannot separate analytes efficiently
52 from the complex samples, the development of selective adsorbents is necessary to apply in the
53 complex samples.

54 It is well known that molecularly imprinted polymers (MIPs) have been widely applied in
55 selective enrichment of organic compounds in complex samples. However, MIPs is not suitable
56 for ionic heavy metals. The preparation of ion imprinting polymers (IIPs) is similar to that of MIP,
57 which is obtained by chelating metal ions and ligands atoms, and then polymerizing with
58 polymer monomer. The combination and breakdown of the coordinate bond between metal ions
59 and ligands can be controlled by changing medium conditions. Currently, the main preparation
60 methods of IIPs are bulk polymerization, in-situ polymerization, precipitation polymerization and
61 suspension polymerization and so on. Although these methods possess the advantages of high
62 selectivity, some disadvantages were suffered, such as the heterogeneous distribution of the
63 binding sites, embedding of most binding sites, and poor site accessibility for target ions. To

64 overcome the above shortcomings, the surface imprinting polymerization has gotten wide
65 attention. So far, the surface imprinting polymers which take Pb^{2+} ,⁵ Ag^+ ,⁹ Cu^{2+} ,¹⁰ Hg^{2+} ¹¹ and
66 other metal ions as templates have been successfully prepared, bearing the advantages of high
67 selectivity, high adsorption capacity as well as fast combination capability.

68 Sol-gel method is the typical representative of the surface imprinting method. Namely, under
69 the effect of an appropriate catalyst (acid, alkali and neutral), inorganic or metal alkoxide can
70 capture oxides and other solid compound through hydrolysis, polymerization, aging and drying
71 steps. In sol-gel method, the most widely used crosslinking agent is alkoxy silane, especially
72 tetramethoxysilane (TMOS)¹²⁻¹⁴ and tetraethoxysilane (TEOS). Templates and the functional
73 monomer are mainly combined with non-covalent bond, including hydrogen bonds,
74 metal-ligands conjugation, ionic bond, hydrophobic function, the van der Waals force and so on.
75¹⁵

76 Although copper is one of the essential trace elements in the human body, intolerable amount
77 of copper can do great harm to human health and cause serious illness, such as nausea, vomiting,
78 weight loss, dehydration, sluggish and anorexia. Few researches on preparing ion-imprinted
79 materials for extraction of copper ions from complex samples have been reported.¹⁶ In this work,
80 a core-shell magnetic ion-imprinted polymer (c-MMWCNTs-SiO₂-IIP) based on c-MMWCNTs
81 was synthesized for the first time with surface imprinting technique. During the preparation
82 process, c-MMWCNTs-SiO₂-IIP was prepared by sol-gel method using c-MMWCNTs-SiO₂ as
83 the core, copper ion as the templates, 3-ammonium propyltriethoxysilane (APTES) as the
84 functional ligand, and tetraethylorthosilicate (TEOS) as the cross-linker. The obtained product
85 was explored for the copper ion adsorption behavior and selectivity, and applied in the extraction
86 and determination of copper ions in herbal medicine.

87 **2 Materials and methods**

88 **2.1 Materials and instruments**

89 Multi-walled carbon nanotubes (diameter 40-60 nm, length 5-15 μm) were purchased from

90 Shenzhen Nanotechnologies Port Company, Ltd., China; Ferric chloride hexahydrate
91 ($\text{FeCl}_3 \cdot 6\text{H}_2\text{O}$) was obtained from Yufeng Chemical Reagents Company (Changsha, China);
92 PEG-10000, ethylene glycol (EG), diethylene glycol (DEG), tetraethoxysilane and pentahydrate
93 copper sulfate ($\text{CuSO}_4 \cdot 5\text{H}_2\text{O}$) were purchased from Aladdin; Sodium diethyl dithiocarbamate
94 (DDTC) was obtained from Tingxin Chemical Reagents Company (Shanghai, China);
95 3-ammonium propyltriethoxysilane (APTES) was obtained from Diomand New Materials of
96 Chemical Inc. (Hubei, China); Cetyl trimethyl ammonium bromide (CTAB) was obtained from
97 Lingfeng Chemical Reagent company, Ltd. (Shanghai, China). All the reagents used in the
98 experiments were of analytical grade. The whole process was conducted in deionized (DI) water.

99 The magnetic field was applied by placing a commercial NdFeB magnet (an alloy of
100 neodymium, iron and boron; 1 cm high and 2 cm in diameter). UV-Vis absorption was
101 characterized by UV1800 UV-Vis spectrophotometer (Shimadzu Corporation, Japan). The size
102 and morphology of the as-synthesized materials were characterized by S-3000 scanning electron
103 microscopy (SEM, Hitachi Corporation, Japan). The surface groups on the as-synthesized
104 materials were measured with a 8400s FTIR spectrometer (Shimadzu Corporation, Japan). The
105 experiments were performed by GFA-EX7i flame atomic absorption spectrometer (FAAS)
106 (Shimadzu, Japan).

107 **2.2 The determination of Cu(II) in aqueous solution**

108 DDTC is selected as the chelating reagent because of the second highest stability constant of
109 Cu(II)-DDTC complex, compared with the stability constants of the other DDTC-metal
110 complexes.¹⁷ The theoretical stoichiometry of DDTC/Cu(II) was 2:1 and the detection
111 wavelength was 454 nm. Since Cu(II)-DDTC complex is a kind of metal complex with low
112 water-solubility, nonionic surfactant CTAB was added to increase the solubility of Cu(II)-DDTC
113 complex in this work. The calibration was performed by using six Cu(II) standards at different
114 concentrations in the range of 0 to 7.0 mg/L. The obtained linear regression equations and
115 correlation coefficients (R^2) for Cu(II) were $A = 0.0990C + 0.0557$ and $R^2 = 0.9987$,

116 correspondingly, where A was the absorbance of the Cu(II) standards and C was the
117 concentrations of Cu(II) added with the unit of mg/L. The relatively standard deviations (RSD%)
118 of intra-day and inter-day precisions taken at the concentration of 3.0, 5.0, 7.0 mg/L were all less
119 than 3%. The recoveries of Cu(II) in aqueous samples ranged from 98.7%±2.8% to
120 100.3%±2.2% (n=6). The limit of detection (LOD) of the proposed method was studied under the
121 optimal experimental conditions. According to the experimental results the LOD of Cu(II) is 1.15
122 µg/L.

123 **2.3 Synthesis of c-MMWCNTs-SiO₂**

124 c-MMWCNTs was obtained according to the previous work reported in our lab.¹⁸ 1.0 g
125 c-MMWCNTs were dispersed in the mixture of 8 mL DI water, 40 mL methanol and 0.5 mL
126 ammonia solution (30%, m/v) and sonicated for 0.5 h. Then, after 15 min continuous mechanical
127 stirring, 0.5 mL TEOS was added into the mixture and reacted at room temperature (25 °C) for
128 12 h. The product can be separated by an extra magnetic field, and then dispersed in Dimethyl
129 Formamide to remove the remaining TEOS. At last, the obtained c-MMWCNTs-SiO₂ was
130 washed by DI water and methanol consecutively, and finally dried in vacuum at 65 °C for 12 h.

131 **2.4 Synthesis of c-MMWCNTs-SiO₂-IIP**

132 0.5 g c-MMWCNTs-SiO₂ was accurately weighed and sonicated in 60 ml methanol to get the
133 mixed suspension A. 2 mmol CuSO₄·5H₂O (0.5 g) and 3.4 mmol CTAB (0.62 g) were accurately
134 weighed, mixed with 36.0 ml DI water and then added into 50 ml conical flask to dissolve by
135 heating. Then 2.0 ml APTES was added to form the blue flocculent precipitate which was
136 dissolved by continuous heating. The obtained solution was named as B. Solution B and 0.7 ml
137 TEOS were added consecutively into suspension A which was put on the mechanical stirring
138 apparatus with the rotating speed of 1500 rpm firstly. The mixed solution was heated in the oil
139 bath at 60°C for 6 h. The obtained copper ion imprinted polymer was washed with DMF to
140 remove the excess of TEOS. Then DI water and methanol were used to wash three times
141 consecutively to remove the excess DMF. Finally the washing process for the loaded polymers

142 was repeated with CH₃OH-0.1 M HNO₃ (volume ratio: 49:1) to remove the templates until the
143 copper ions could not be detected anymore by DDTC. The prepared c-MMWCNTs-SiO₂-IIP was
144 washed by DI water and methanol consecutively, and then dried in vacuum at 65°C for 12 h. The
145 schematic preparation process of c-MMWCNTs-SiO₂-IIP was shown in Fig.1.

146 At the same time, the non-ion imprinted polymer (c-MMWCNTs-SiO₂-NIP) was prepared as a
147 control test. The schematic preparation process was just followed the above steps without adding
148 copper ions.

149 According to the above method, carboxyl carbon nanotubes (c-MWCNTs) and magnetic
150 ferroferric oxide nanoparticles (MNP) were also used as the core, and the corresponding ion
151 imprinted polymers and non-ion imprinted polymer were prepared, respectively
152 (c-MWCNTs-SiO₂-IIP, c-MWCNTs-SiO₂-NIP, MNP-SiO₂-IIP and MNP-SiO₂-NIP).

153 **2.5 Batch adsorption experiments**

154 Batch adsorption experiments of c-MMWCNTs-SiO₂-IIP and c-MMWCNTs-SiO₂-NIP were
155 performed in deionized water. Respective polymers (10 mg) were shaken with 10 mL of
156 deionized water (pH= 7.5) spiked with Cu(II) at room temperature for 4 h with 1500 rpm by
157 THZ-C Constant temperature shaker. Then the polymers were collected by an external
158 magnetic force. The supernatant was analyzed by UV-1800 spectrophotometer (Shimadzu, Japan).

159 The amount of Cu(II) adsorbed by the polymers was calculated according to the following
160 formula:

$$161 \quad Q = \frac{(C_0 - C)V}{1000W} \quad (1)$$

162 where Q is the adsorbed amount of Cu(II) (mg/g); C₀ and C are the initial and final
163 concentration of Cu(II) (μg/mL), respectively; V is the volume of solution (mL); W is the
164 amount of polymer (g).

165 **2.6 The determination of residual Cu(II) in the herbal medicine extractions**

166 The samples analyzed consisted of different matrices (rhizome of *Salvia Miltiorrhiza*,
167 herbaceous stem of *Herba Ephedrae*, flowers of *Lonicera Japonica* and root of *Radix Astragali*).

168 Four different commercial TCMs in a total of 20 samples were collected from several herbal
169 shops in 2012. All samples were milled (particle size about 2 mm) and stored at -18°C prior to
170 analyses for the determination of residual Cu(II). The traditional Chinese medicines (TCM) were
171 digested by dry ashing method. The main advantages of the dry ashing method were the lower
172 blank levels, improved (lower) background current and its ability to handle considerably larger
173 amounts of sample. Sample preparation was carried out according to Chinese Pharmacopoeia
174 (2010 version). Accurately weighed 0.5 g of test samples into crucible and heated with low
175 temperature to smokeless, and then incandescenced in furnace for 6 hours at 500°C . The ashes were
176 extracted by 15 ml 8 mol/L HNO_3 for 0.5 h, then filtrated through $0.45\ \mu\text{m}$ filter membrane, After
177 acidification with HNO_3 , pH of the samples were adjusted to neutral before determination by
178 GFA-EX7i flame atomic absorption spectrometer (FAAS) (Shimadzu, Japan).

179 **3. Results and discussion**

180 **3.1 Characteristics**

181 Fig.2 showed the particles sizes of c-MMWCNTs-SiO₂, c-MMWCNTs-SiO₂-NIP and
182 c-MMWCNTs-SiO₂-IIP under the same visual field. As shown in Fig. 2A, Fe₃O₄ nanoparticles
183 were deposited onto the surfaces of the c-MWCNTs. As shown in Fig.2B and 2C, the diameters
184 of c-MMWCNTs-SiO₂-NIP and c-MMWCNTs-SiO₂-IIP were increased, indicating that a
185 polymer layer might have been successfully coated on the surfaces of c-MMWCNTs-SiO₂.

186 8400s FT-IR spectroscopy (Shimadzu, Japan) was used to study the chemical structure of
187 c-MMWCNTs (A), c-MMWCNTs-SiO₂-NIP (B) and c-MMWCNTs-SiO₂-IIP (C). The results
188 were shown in Fig.3. A strong peak at $3400\text{-}3500\ \text{cm}^{-1}$ corresponding to the stretching O-H was
189 observed in all the samples.¹⁹ The strong peak at $620\ \text{cm}^{-1}$ belonged to the stretching Fe-O,
190 which indicated the Fe₃O₄ particles were encapsulated inside of c-MMWCNTs-SiO₂-IIP. The
191 peaks at $1650\ \text{cm}^{-1}$ and $950\text{-}980\ \text{cm}^{-1}$ corresponded to the in-plane bending vibration of C-NH₂
192 and asymmetric stretching vibration of Si-OH, respectively. It was notable in Fig.3C that the
193 asymmetric stretching vibration peaks of O-Si-O at $1000\text{-}1250\ \text{cm}^{-1}$ and Si-O-C at $1380\ \text{cm}^{-1}$ in

194 c-MMWCNTs-SiO₂-IIP were stronger than that of c-MMWCNTs-SiO₂-NIP, which indicated the
195 formation of O-Si-O polymer.

196 **3.2 Adsorption behaviors of imprinted polymers**

197 **3.2.1 Adsorption capacity**

198 Since c-MMWCNTs were consisted of c-MWCNTs and MNP, IIPs corresponding to
199 c-MMWCNTs, c-MWCNTs and MNP were prepared and investigated of adsorption capacity.
200 The adsorption capacity of IIPs toward Cu(II) was investigated by batch experiments. Fig.4A is
201 Cu(II) isothermal adsorption behavior on c-MMWCNTs-SiO₂-IIP (c-MWCNTs-SiO₂-IIP or
202 MNP-SiO₂-IIP). It can be seen that the adsorption capacity of c-MMWCNTs-SiO₂-IIP (or
203 c-MWCNTs-SiO₂-IIP, MNP-SiO₂-IIP) increased with the increasing initial concentration of Cu(II)
204 solution. When the initial concentration increased to a certain degree, the adsorption capacity
205 tended into balance. The order of the adsorption capacity for three adsorbents was found as
206 follows, c-MWCNTs-SiO₂-IIP > c-MMWCNTs-SiO₂-IIP > MNP-SiO₂-IIP with the amount of
207 42.8 mg/g, 36.6 mg/g and 18.5 mg/g respectively, which might be attributed to their specific
208 surface area.

209 Although the adsorption capacity of c-MMWCNTs-SiO₂-IIP was slightly lower than that of
210 c-MWCNTs-SiO₂-IIP, c-MMWCNTs-SiO₂-IIP can quickly be separated from the solution due to
211 the magnetic performance, which bringing great convenience to the experiment. Therefore,
212 c-MMWCNTs-SiO₂-IIP was selected as the further research object in this study. Compared the
213 adsorption capacity of c-MMWCNTs-SiO₂-IIP with that of c-MMWCNTs-SiO₂-NIP, the result
214 was shown in Fig.4B. The adsorption capacities of c-MMWCNTs-SiO₂-IIP was 36.6 mg/g, which
215 was nearly three times more than that of c-MMWCNTs-SiO₂-NIP 13.1 mg/g. This can be
216 explained that the presence of the functional group of -CH₂-NH₂ in the selective hole of
217 c-MMWCNTs-SiO₂-IIP can absorb more Cu(II) by coordination effect.²⁰

218 In this experiment, c-MMWCNTs-SiO₂-IIP was prepared by the surface imprinting method,
219 and Langmuir equation is suitable for monolayer adsorption on a surface, thus in order to further

220 discuss the adsorption behavior of Cu(II) on c-MMWCNTs-SiO₂-IIP, Langmuir isotherm model
221 was used to analyse the isothermal adsorption data obtained from Fig.4B. The Langmuir equation
222 was expressed as follow:

$$223 \quad \frac{1}{q_e} = \frac{1}{Q_{\max}} + \frac{1}{bQ_{\max} C_e} \quad (2)$$

224 where q_e (mg/g) is the equilibrium adsorbed amount of Cu(II), Q_{\max} (mg/g) is the maximum
225 adsorption capacity, C_e (mg/L) is the equilibrium concentration, and b (L/mg) is the adsorption
226 equilibrium constant. The correlation coefficient (R^2) and the maximum adsorption capacity
227 (Q_{\max}) was calculated as 0.997 and 42.2 mg/g (shown in Fig.5.).

228 **3.2.2 Adsorption kinetic**

229 Adsorption kinetic experiments of Cu(II) on c-MMWCNTs-SiO₂-IIP and
230 c-MMWCNTs-SiO₂-NIP were conducted in aqueous solution by a batch system. Briefly, 20.0 mg
231 of the imprinted sorbent was added to 50 mL of 100 µg/mL Cu(II) aqueous solution at pH 7.0. It
232 can be seen that a much higher adsorption capacity was achieved on c-MMWCNTs-SiO₂-IIP
233 shown in Fig.6. Saturation adsorption of 40.4 mg/g can be obtained within 50 min, which can be
234 attributed to the high coordination effect between -CH₂-NH₂ and Cu(II). However, the saturation
235 adsorption of c-MMWCNTs-SiO₂-NIP, which was obtained within 120 min, was obviously
236 smaller than that of c-MMWCNTs-SiO₂-IIP, indicating the good affinity to Cu(II) of
237 c-MMWCNTs-SiO₂-IIP.

238 Moreover, the pseudo first-order and pseudo second-order kinetic models were used to
239 investigate the kinetic mechanism driving Cu(II) adsorption further.^{21,22} The pseudo-first order
240 equation is given as follows:

$$241 \quad \log(q_e - q_t) = \log(q_e) - \frac{k_1 t}{2.303} \quad (3)$$

242 where k_1 is the rate constant of first order sorption (min^{-1}); q_e is the amount of solute sorbed at
243 equilibrium (mg/g); q_t is the amount of solute sorbed on the surface of the sorbent at time t
244 (mg/g).

245 The pseudo-second order equation is given as follows:

$$246 \left(\frac{t}{q_t} \right) = \left(\frac{1}{k_2 q_e^2} \right) + \left(\frac{t}{q_e} \right) \quad (4)$$

247 where k_2 is the rate constant for the pseudo second-order adsorption of Cu(II) (g/mg min), and all
248 other variables in pseudo-second order equation are the same with pseudo-first order equation as
249 described above.

250 Fig.7 was the plots of the linearized form of pseudo first-order and pseudo-second order model.
251 The calculated equilibrium adsorption capacity ($Q_{e,cal} = 53.2$ mg/g) was obtained from
252 pseudo-first-order with a low correlation coefficient ($R^2 = 0.965$). Whereas, the calculated
253 equilibrium adsorption capacities ($Q_{e,cal} = 46.5$ mg/g) estimated from pseudo-second-order
254 kinetic model with a high correlation coefficient ($R^2 = 0.985$), is relatively close to the maximum
255 adsorption capacity ($Q_{eq} = 42.2$ mg/g). Therefore, the adsorption system of
256 c-MMWCNTs-SiO₂-IIP toward Cu(II) was better fit to pseudo-second order model. And this
257 adsorption mechanism was predominant for the ion-imprinted adsorbent system based on the
258 assumption that the rate-limiting step might be chemical sorption between chemical binding sites
259 on the surface of c-MMWCNTs-SiO₂-IIP and Cu(II).⁵

260 3.2.3 Selectivity

261 The selectivity of c-MMWCNTs-SiO₂-IIP toward Cu(II) was evaluated by competitive
262 adsorption in the presence of various competitive metal ions. A mixture of Pb(II), Cu(II) and
263 Zn(II) was added into deionized water to obtain 25ml of 100 µg Pb(II), 100 µg Zn(II) and 100 µg
264 Cu(II). After a competitive adsorption equilibrium reached for 4 h, the concentration of Pb(II),
265 Zn(II) and Cu(II) in the remaining samples were detected by FAAS. The following equations
266 were used to quantify the selectivity of c-MMWCNTs-SiO₂-IIP :²³

267 Distribution ratio (mL/g),

$$268 K = \frac{Q}{C_e} \quad (5)$$

269 where Q is the adsorption capacity (mg/g).

270 Selectivity factor ,

$$271 \quad \alpha = \frac{K_t}{K_c} \quad (6)$$

272 where K_t and K_c are the distribution ratio Cu(II) and Pb(II) or Zn(II), respectively.

273 Relative selectivity factor ,

$$274 \quad \beta = \frac{\alpha_i}{\alpha_n} \quad (7)$$

275 where α_i and α_n are the selectivity factor of c-MMWCNTs-SiO₂-IIP and c-MMWCNTs-SiO₂-NIP.

276 Since Zn(II) and Pb(II) can be determined directly in the aqueous solution when mixed with
277 Cu(II), in the selectivity experiment the concentration of the ions were measured by FAAS. The
278 absorbance (A) of Cu(II), Zn(II) and Pb(II) stock solutions were determined at 324.8 nm, 213.8
279 nm and 283.3 nm by FAAS, respectively. Table 1 listed the distribution ratio, selectivity factor
280 and relative selectivity factor of c-MMWCNTs-SiO₂-IIP and c-MMWCNTs-SiO₂-NIP for Cu(II).
281 As shown in Table 1, the distribution ratio and selectivity factor of c-MMWCNTs-SiO₂-IIP were
282 much greater than that of c-MMWCNTs-SiO₂-NIP, showing that c-MMWCNTs-SiO₂-IIP born
283 higher selectivity for Cu(II). Moreover, the distribution ratio of c-MMWCNTs-SiO₂-IIP for Cu(II)
284 was much higher than those for other ions. The results implied that the imprinted cavities and
285 specific binding sites in a predetermined orientation were formed. Cu(II), Zn(II) and Pb(II) had
286 the same charge, and Cu(II) and Zn(II) had the similar atomic radius, but higher selectivity of
287 c-MMWCNTs-SiO₂-IIP for Cu(II) might be attributed to the different chelation forces between
288 nitrogen atoms in APTES toward various ions. Relative selectivity factor (β) represented relative
289 affinities of imprinting ions. $\beta(\text{Cu(II)/Zn(II)})$ and $\beta(\text{Cu(II)/Pb(II)})$ of c-MMWCNTs-SiO₂-IIP
290 were 38.5 and 34.5, respectively. It can be referred that the affinity order of
291 c-MMWCNTs-SiO₂-IIP toward Cu(II), Zn(II) and Pb(II) was Cu(II) > Zn(II) > Pb(II).

292 **3.2.4 Effect of pH on the adsorption and desorption of Cu(II)**

293 It is well known that pH plays an important role in the adsorption performance of the
294 imprinted polymer toward different ions .²⁴Since Cu(II) started precipitating when the pH of the
295 solution was bigger than 7.0 ,²⁵ the effect of pH on the adsorption of c-MMWCNTs-SiO₂-IIP
296 toward Cu(II) was studied with varying pH from 1.0 to 7.0 and the results were presented in
297 Fig.8. The results showed that the adsorption percentage of Cu(II) increased with the increasing
298 pH of the aqueous solution from 1.0 to 7.0. At lower pH, the adsorption capacity of Cu(II) is very
299 low due to two reasons. One is the protonation of -CH₂-NH₂, which might hinder the
300 complexation between Cu(II) and the functional groups;²⁶The second one is the over acidity
301 might hydrolyze the O-Si-O-Si bond structure in the c-MMWCNTs-SiO₂-IIP polymer, thus
302 affecting its absorption capacity.

303 Since the acid condition can decrease the adsorption of Cu(II) on c-MMWCNTs-SiO₂-IIP, low
304 pH could contribute to the elution. However, the volume of the polymers decreased gradually
305 when washed by CH₃OH-0.1 M HNO₃ (9:1, v/v) mixture solution during the elution process. It
306 can be referred that the coating layer might be destroyed. Thus, the c-MMWCNTs-SiO₂-IIP
307 polymer loaded with Cu(II) should be eluted with suitable eluent. To find the suitable eluent, the
308 loaded c-MMWCNTs-SiO₂-IIP polymers were washed with CH₃OH-0.1 M HNO₃ mixture
309 solution of different acidity (9:1 or 49:1, v/v). When washed by CH₃OH-0.1 M HNO₃ (9:1, v/v)
310 mixture solution, the supernatant was clear with no Cu(II) after eluting for about 6 or 7 times, but
311 the volume of the polymer decreased significantly. When washed by CH₃OH-0.1 M HNO₃ (49:1,
312 v/v), the supernatant was clear with no Cu(II) after eluted for about 20 to 30 times, and the
313 volume of the polymer showed no obvious change. From the apparent phenomenon, it can be
314 speculated that CH₃OH-0.1 M HNO₃ (49:1, v/v) might be the suitable eluent. To support the
315 above-mentioned conclusion, the polymers washed by two eluents were characterized by SEM
316 and the results were shown in Fig.9. It was obviously that the volume of c-MMWCNTs-SiO₂-IIP
317 eluted by CH₃OH-0.1 M HNO₃ (49:1, v/v) was bigger than that washed by CH₃OH-0.1 M HNO₃
318 (9:1, v/v), indicating that strong acid can destroy the structure of c-MMWCNTs-SiO₂-IIP.

319 Therefore, the acidity of the solutions should be strictly controlled during the process of
320 experiment.

321 **3.3 Application**

322 Under the optimum conditions, the imprinted polymers were used for the extraction of Cu(II)
323 from herbal medicines spiked with various amounts of Cu(II). After incubation with herbal
324 medicines extractions, IIP were eluted with CH₃OH-0.1 M HNO₃ (49:1, v/v) mixture solution,
325 the concentration of Cu(II) in the elution was detected using FAAS. The linear range of the
326 magnetic solid phase extraction coupled with FAAS method was established to be 0.70-100.00
327 µg/g. The correlation coefficient of the calibration graphs is 0.9974. The relatively standard
328 deviations (RSD%) of intra-day and inter-day precisions taken at the concentration of 20.00 and
329 50.00 µg/g were all less than 3%. The detection limit (LOD) of the presented solid phase
330 extraction study was calculated under optimal experimental conditions after application of the
331 preconcentration procedure to blank solutions. The detection limits, defined as the concentration
332 equivalent to three times the standard deviation (N = 12) of the reagent blank were found as 0.21
333 µg/g.

334 As shown in Table 2, high recoveries ranged from 95.6% to 108.4% in the all tested
335 concentration of Cu(II), which indicated that IIP showed a high effectivity for extracting Cu(II)
336 from herbal medicine extractions. According to green trade standards of importing medicinal
337 plants and the preparations, the total amount of heavy metals should be less than 20.0 µg/g, and
338 Cu(II) less than 20.0 µg/g. Experimental results showed that Cu(II) in the herbal medicines
339 extraction was less than 20.0 µg/g, which is according with the regulation. Reusability of
340 c-MMWCNTs-SiO₂-IIP is one of key factors in evaluating the performance of the adsorption
341 materials. In order to investigate the reusability and stability of c-MMWCNTs-SiO₂-IIP
342 adsorption-desorption cycle was repeated five times by using the same imprinted materials. The
343 results showed that c-MMWCNTs-SiO₂-IIP was stable in operation process, which could be used
344 for five cycles with lost of less than 7.2% of Cu(II) recoveries on average.

345

346 **4. Conclusions**

347 In our work, a magnetic surface ion-imprinted polymer based on c-MMWCNTs was
348 prepared successfully by a sol-gel process. The obtained c-MMWCNTs-SiO₂-IIP exhibited high
349 selectivity toward Cu(II) with the relative selectivity factor over 34.5 in the presence of Cu(II),
350 Zn(II) and Pb(II). When the magnetic adsorbent was used in herbal medicine extractions, good
351 recoveries (>95.0%) for Cu(II) were obtained under the optimized conditions. The magnetic
352 imprinted adsorbent can be applied to rapid extraction of Cu(II) from herbal medicine extractions,
353 which can lower the influence of the interference matrix, thereby optimize the detection limit of
354 detection methods. Also, the magnetic performance of c-MMWCNTs-SiO₂-IIP did not need
355 column packing when used in the M-SPE, thereby lessening the column pressure and increasing
356 the effective contact area which can improve the extraction efficiency. Moreover, the reusability
357 and stability of c-MMWCNTs-SiO₂-IIP for five circles make it a promising adsorbent in selecting
358 heavy metal ions from complex samples.

359 **Acknowledgements**

360 This work was supported by National Natural Science Foundation of China (No. 21207061),
361 Guizhou Provincial Natural Science Foundation of China (No. J20122288) and the National
362 Major Project of Science and Technology Ministry of China (No. 2012ZX07204-001).

363

364 **References**

- 365 1. X. Yuan, R. L. Chapman and Z. Wu, *Phytochemical Analysis*, 2011, 22, 189-198.
366 2. Y.-K. Tsoi, Y.-M. Ho and K. S.-Y. Leung, *Talanta*, 2012, 89, 162-168.
367 3. B. Godlewska-Żyłkiewicz, B. Leśniewska and I. Wawreniuk, *Talanta*, 2010, 83, 596-604.
368 4. J. Manzoori, M. Amjadi and M. Darvishnejad, *Microchimica Acta*, 2012, 176, 437-443.
369 5. M. Zhang, Z. Zhang, Y. Liu, X. Yang, L. Luo, J. Chen and S. Yao, *Chemical Engineering*
370 *Journal*, 2011, 178, 443-450.
371 6. R. Gao, X. Kong, F. Su, X. He, L. Chen and Y. Zhang, *Journal of Chromatography A*, 2010,
372 1217, 8095-8102.
373 7. J.-L. Gong, B. Wang, G.-M. Zeng, C.-P. Yang, C.-G. Niu, Q.-Y. Niu, W.-J. Zhou and Y. Liang,
374 *Journal of Hazardous Materials*, 2009, 164, 1517-1522.

- 375 8. C. Chen, J. Hu, D. Shao, J. Li and X. Wang, *Journal of Hazardous Materials*, 2009, 164,
376 923-928.
- 377 9. L. Fan, C. Luo, Z. Lv, F. Lu and H. Qiu, *Journal of Hazardous Materials*, 2011, 194,
378 193-201.
- 379 10. Y. Zhan, X. Luo, S. Nie, Y. Huang, X. Tu and S. Luo, *Industrial & Engineering Chemistry*
380 *Research*, 2011, 50, 6355-6361.
- 381 11. H. R. Rajabi, M. Roushani and M. Shamsipur, *Journal of Electroanalytical Chemistry*, 2013,
382 693, 16-22.
- 383 12. V. G. Gavalas, R. Andrews, D. Bhattacharyya and L. G. Bachas, *Nano Letters*, 2001, 1,
384 719-721.
- 385 13. R. D. Makote and S. Dai, *Analytica Chimica Acta*, 2001, 435, 169-175.
- 386 14. Z. Zhang, H. Zhang, Y. Hu and S. Yao, *Analytica Chimica Acta*, 2010, 661, 173-180.
- 387 15. S. Daniel, R. S. Praveen and T. P. Rao, *Analytica Chimica Acta*, 2006, 570, 79-87.
- 388 16. X. Luo, S. Luo, Y. Zhan, H. Shu, Y. Huang and X. Tu, *Journal of Hazardous Materials*, 2011,
389 192, 949-955.
- 390 17. M. T. Joanna Szpunar-Lobinska, *Anal. Sci.*, 1990, 6, 415-419.
- 391 18. D. Xiao, P. Dramou, H. He, L. A. Pham-Huy, H. Li, Y. Yao and C. Pham-Huy, *Journal of*
392 *Nanoparticle Research*, 2012, 14, 1-12.
- 393 19. Y.-K. Lu and X.-P. Yan, *Analytical Chemistry*, 2003, 76, 453-457.
- 394 20. P.-G. Su, F.-C. Hung and P.-H. Lin, *Materials Chemistry and Physics*, 2012, 135, 130-136.
- 395 21. C.-Y. Chen, C.-Y. Yang and A.-H. Chen, *Journal of Environmental Management*, 2011, 92,
396 796-802.
- 397 22. M. A. Tofighy and T. Mohammadi, *Journal of Hazardous Materials*, 2011, 185, 140-147.
- 398 23. D. Xiao, P. Dramou, N. Xiong, H. He, H. Li, D. Yuan and H. Dai, *Journal of*
399 *Chromatography A*, 2013, 1274, 44-53.
- 400 24. M. T. Jafari, B. Rezaei and B. Zaker, *Analytical Chemistry*, 2009, 81, 3585-3591.
- 401 25. A. Paulson and D. Kester, *J Solution Chem*, 1980, 9, 269-277.
- 402 26. Z. Wang, G. Wu, M. Wang and C. He, *Journal of Materials Science*, 2009, 44, 2694-2699.

403

404

405

Figure Captions

406

407 **Fig. 1** Schematic expression of synthesis of c-MMWCNTs-SiO₂-IIP

408 **Fig. 2** SEM images of c-MMWCNTs -SiO₂ (A), c-MMWCNTs -SiO₂-NIP (B) and c-MMWCNTs -SiO₂-IIP (C).

409 **Fig.3** FT-IR spectra of c-MMWCNTs (A), c-MMWCNTs-SiO₂-NIP (B) and c-MMWCNTs-SiO₂-IIP (C).

410 **Fig.4** The adsorption isotherms of Cu(II) on three kinds of IIPs (A) and c-MMWCNTs-SiO₂-IIP
411 (c-MMWCNTs-SiO₂-NIP) (B)

412 **Fig.5** Langmuir isothermal model for Cu²⁺ adsorption on c-MMWCNTs-SiO₂-IIP.

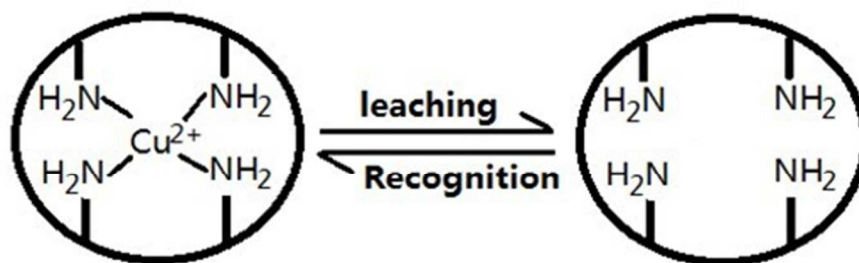
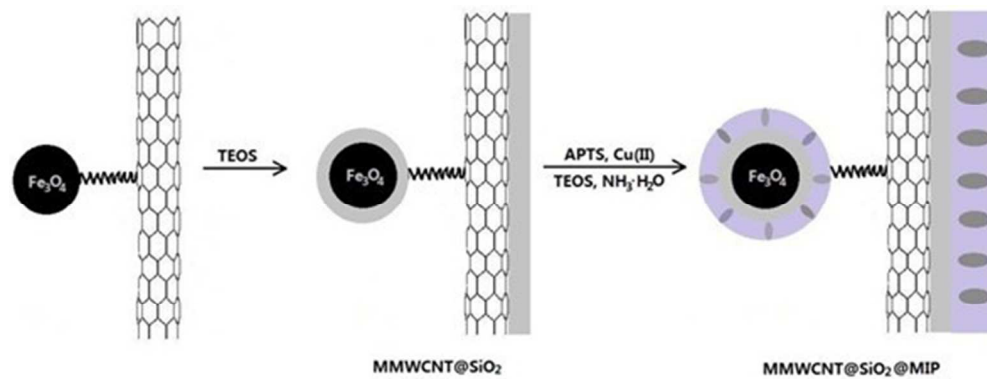
413 **Fig.6** Adsorption kinetic curves of c-MMWCNTs-SiO₂-IIP and c-MMWCNTs-SiO₂@NIP.

414 **Fig.7** Pseudo-first-order (A) and pseudo-second-order (B) kinetic models for adsorption of Cu(II) onto H₂-MNP.

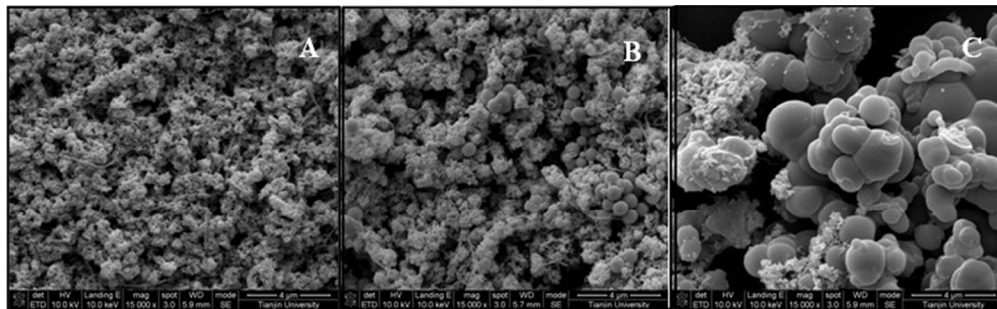
415 **Fig.8** Effect of pH on adsorption capacity of c-MMWCNTs-SiO₂-IIP.

416 **Fig.9** The SEM images of c-MMWCNTs-SiO₂-IIP washed by different proportions of CH₃OH-0.1 M HNO₃: 49:1
417 (A) and 9:1 (B).

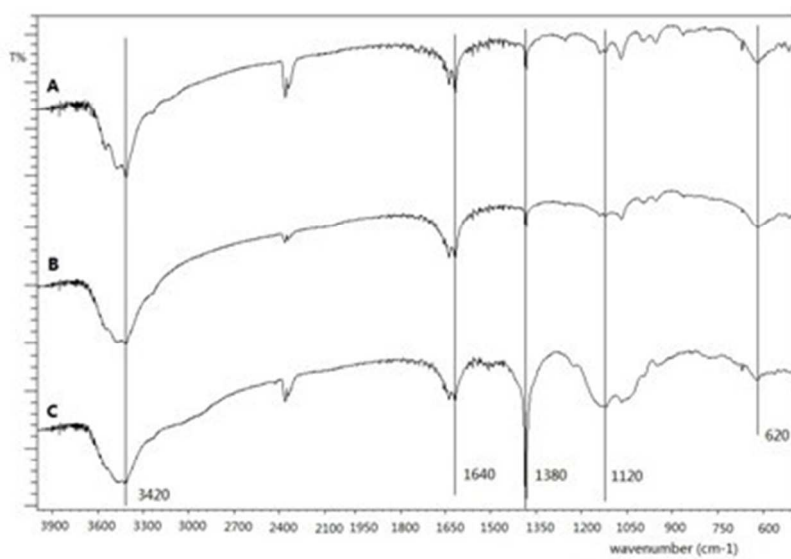
418



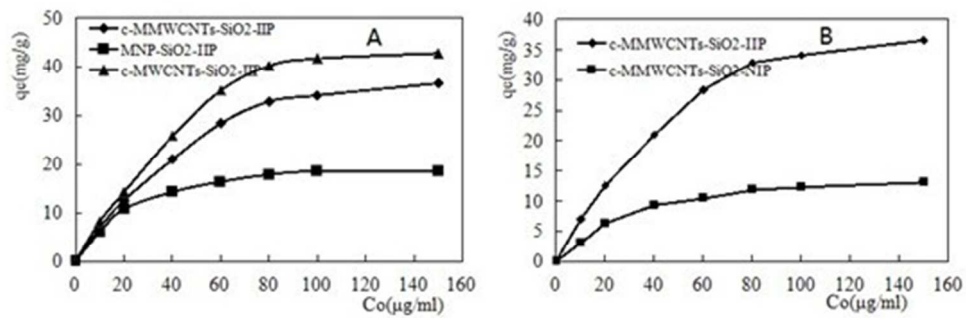
157x125mm (96 x 96 DPI)



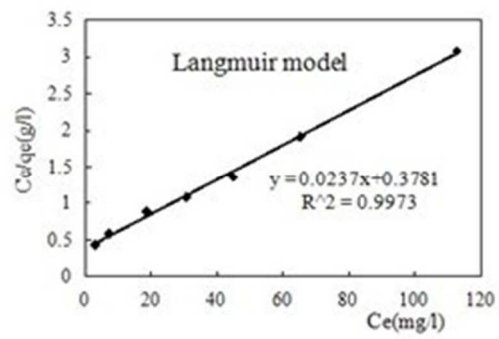
203x62mm (96 x 96 DPI)



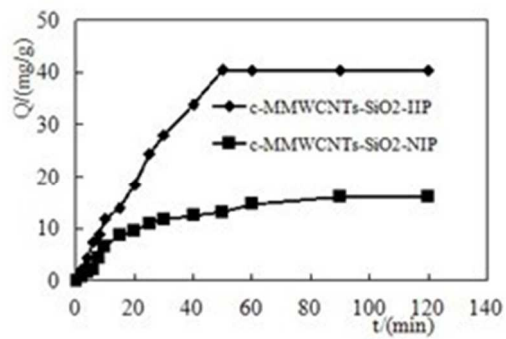
109x77mm (96 x 96 DPI)



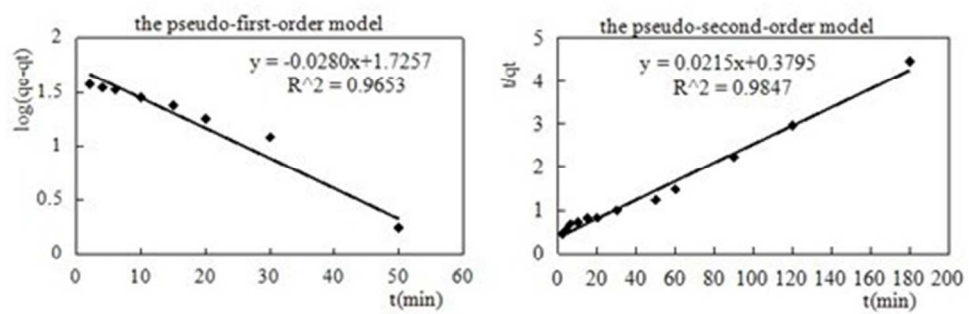
147x51mm (96 x 96 DPI)



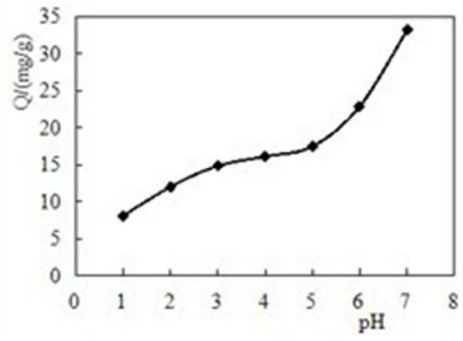
71x47mm (96 x 96 DPI)



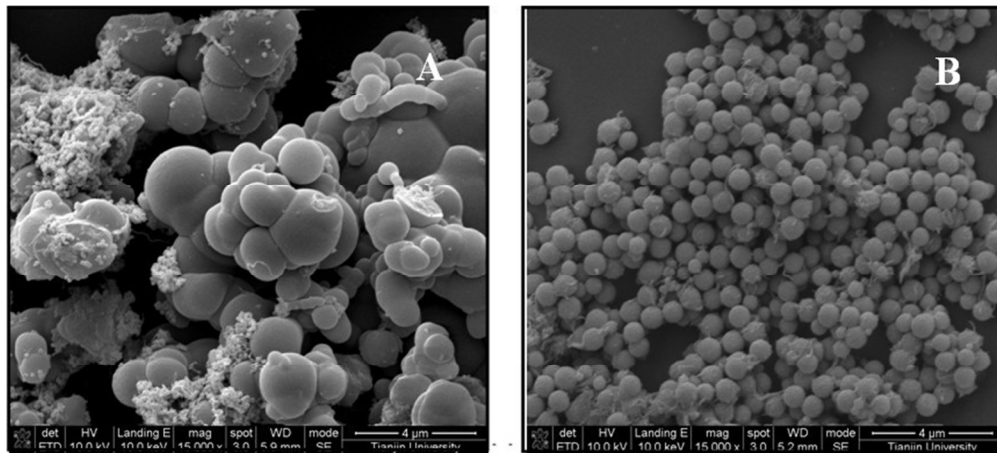
70x50mm (96 x 96 DPI)



141x50mm (96 x 96 DPI)



66x48mm (96 x 96 DPI)



227x102mm (96 x 96 DPI)

Table 1 Distribution ratio, selectivity coefficient and relative selectivity coefficient of c-MMWCNTs-SiO₂-IIP and c-MMWCNTs-SiO₂-NIP

| Metal ions | Ionic charge | Ionic radii (Å) | K(ml/g) | | α | | β |
|------------|--------------|-----------------|----------------------|----------------------|-------|------|------|
| | | | IIP | NIP | IIP | NIP | |
| Cu | 2 | 0.73 | 2.17×10 ⁴ | 5.57×10 ² | - | - | - |
| Zn | 2 | 0.74 | 5.05×10 ² | 4.99×10 ² | 43.0 | 1.12 | 38.5 |
| Pb | 2 | 1.19 | 2.16×10 ² | 1.91×10 ² | 100.6 | 2.92 | 34.5 |

Table 2 Recoveries of Cu(II) in traditional Chinese medicine samples.

| Samples | Added (μg) | Found ($\mu\text{g/g}$, n=4) | Recovery (%) |
|---------------------|-------------------------|--------------------------------|--------------|
| Salvia Miltiorrhiza | 0 | 0.81 ± 0.17^a | -- |
| | 20 | 22.50 ± 0.75^a | 108.4 |
| | 50 | 53.12 ± 1.70^a | 104.5 |
| Herba Ephedrae | 0 | 0.77 ± 0.18^a | -- |
| | 20 | 21.33 ± 0.85^a | 103.7 |
| | 50 | 52.89 ± 1.58^a | 104.7 |
| Lonicera japonica | 0 | BDL | -- |
| | 20 | 19.09 ± 0.40^a | 95.6 |
| | 50 | 49.32 ± 1.49^a | 98.6 |
| Radix Astragali | 0 | BDL | -- |
| | 20 | 20.54 ± 0.62^a | 102.4 |
| | 50 | 50.28 ± 2.53^a | 100.6 |

^a Uncertainty is the standard deviation for four replicate runs.

BDL: below the detection limit